Separation Science and Technology
Publication details, including instructions for authors and subscription information:
http://www.informaworld.com/smpp/title~content=t713708471

Suppression of Osmotic Distillation in Gas Membrane Processes

Z. Shen[a]; L. Zhang[a]; S. Mondal[b]; S. R. Wickramasinghe[b]
[a] Jiangsu Institute of Microbiology, Wuxi, P.R. China [b] Department of Chemical and Biological Engineering, Colorado State University, Fort Collins, CO, USA

To cite this Article Shen, Z. , Zhang, L. , Mondal, S. and Wickramasinghe, S. R.(2008) 'Suppression of Osmotic Distillation in Gas Membrane Processes', Separation Science and Technology, 43: 15, 3813 — 3825
To link to this Article: DOI: 10.1080/01496390802282081
URL: http://dx.doi.org/10.1080/01496390802282081

Separation Science and Technology, 15: 3813–3825, 2008
Copyright © Taylor & Francis Group, LLC
ISSN: 0149-6395 print/1520-5754 online
DOI: 10.1080/01496390802282081

Suppression of Osmotic Distillation in Gas Membrane Processes

Z. Shen,[1] L. Zhang,[1] S. Mondal,[2] and S. R. Wickramasinghe[2]
[1]Jiangsu Institute of Microbiology, Wuxi, P.R. China
[2]Department of Chemical and Biological Engineering,
Colorado State University, Fort Collins, CO, USA

Abstract: Suppression of osmotic distillation of water is important for the commercial scale application of gas membranes. We have equalized the water vapor pressure on either side of the membrane by increasing the temperature of the stream with the lower water vapor pressure. The experimentally determined temperature gradient is many times larger than predicted from water vapor pressure–temperature data. The larger temperature gradient may be explained by considering the heat flux across the membrane. The economic viability of adjusting the temperature of the feed and strip streams to suppresses water vapor transport depends on the additional energy costs involved.

Keywords: Direct contact membrane distillation, gas membranes, hollow fibres, osmotic distillation

INTRODUCTION

Microporous hydrophobic membranes may be used to combine gas absorption and stripping into one unit operation. "Gas membranes" contain gas filled membrane pores while two gas liquid interfaces are stabilized at either surface of the membrane (1–3). A gas membrane process that has been described frequently in the literature is the removal of

Received 14 January 2008; accepted 9 June 2008.

Address correspondence to S. R. Wickramasinghe, Department of Chemical and Biological Engineering, Colorado State University, Fort Collins, CO 80523, USA. Tel.: +1 970 491 5276. Fax: +1 970 491 7369. E-mail: wickram@engr.colostate.edu

cyanide from wastewater (4–7). In this process the wastewater containing cyanide flows on one side of a microporous membrane while the strip solution containing sodium hydroxide flows on the other side. The protonated form of cyanide (prussic acid, HCN) is a weak acid with a pKa of 9.31. Providing the pH of the feed is below about 8.5, the majority of the HCN will be present in the protonated form. Since HCN is volatile it will vaporize, diffuse across the gas filled membrane pores and into the strip solution. In the reactive strip solution it will react to form NaCN:

$$\mathrm{HCN} + \mathrm{NaOH} \rightarrow \mathrm{NaCN} + \mathrm{H_2O}$$

Nondispersive gas absorption/gas stripping using microporous membranes offers a number of advantages over conventional gas absorption/gas stripping (1). The gas and liquid flowrates can be varied over a large range without complications due to flooding and loading. Further, the interfacial area for mass transfer is determined by the membrane porosity and is not affected by the gas or liquid flow rates. From a practical perspective, membrane devices are easily scalable and are modular allowing for flexible operation.

A pilot scale facility for cyanide removal from four industrial wastewater streams using gas membranes has been described by Shen et al. (6). The removal efficiency for cyanide was 99%. The cyanide concentration in wastewater could be reduced to less than 0.5 mg/L. However, during operation, it was observed that water passed from one side of the membrane to the other. Shen et al. noted that the activity of the feed and strip solutions depend on the concentration of dissolved solutes present. This in turn leads to differences in the water vapor pressure on either side of the membrane. Thus water vapor will transfer through the membrane pores down the vapor pressure gradient via a process described in the literature as osmotic distillation.

Transfer of water vapor by osmotic distillation has two main drawbacks for industrial scale operations. If water vapor transfers from the feed to the strip solution, it will lead to dilution of the cyanide in the strip. Since the economic viability of the process often depends on the recovery of the cyanide, the inclusion of an additional step to concentrate the cyanide may be necessary, and could adversely affect the viability of the gas membrane process. Further depending on the direction of water vapor transport the feed or strip tanks will need to be overdesigned. Thus preventing water vapor transfer due to osmotic distillation is of practical significance.

In this study, we have investigated the effect of altering the temperatures of the feed and strip solutions in order to suppress osmotic distillation. The feed and strip solutions consisted of DI water. Various amounts of NaCl were added to the strip solution leading to water vapor transport from the feed to the strip. The strip was then heated and the feed held at 20°C in order to equalize the water vapor pressure on either side of the membrane. Thus by establishing a temperature gradient across the membrane that produces a water vapor pressure gradient in the opposite direction to the gradient due to the different solute activities in the feed and strip solutions, we suppress osmotic distillation of water vapor.

THEORY

Membrane distillation has many similarities to osmotic distillation. In both processes water vapor is transferred through the membrane pores due to a partial pressure gradient. There are various modes of operation for membrane distillation. Figure 1 is a schematic representation of the combined direct contact membrane distillation osmotic distillation process investigated here. The water vapor pressure gradient in osmotic distillation is derived from the difference in the solute concentration in the feed and strip solutions. The applied temperature gradient results in a partial pressure gradient in the opposite direction.

Here our concern is the transport of water vapor during gas membrane processes. Since water vapor is the solvent, the mass transfer resistances in the feed and strip solutions due to the presence of a

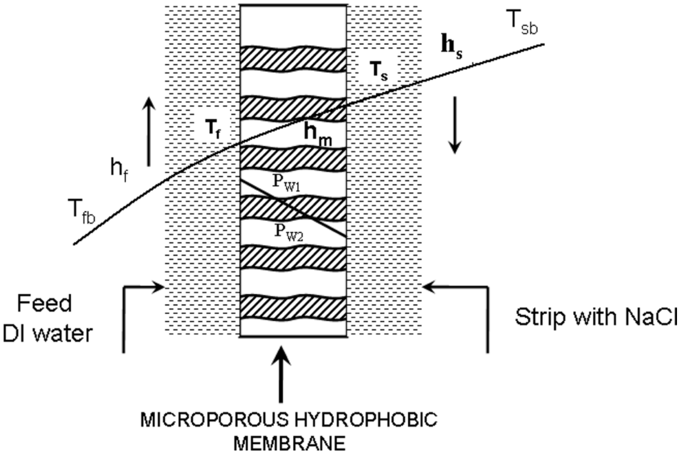

Figure 1. Schematic representation of combined direct contact membrane distillation osmotic distillation system.

concentration boundary layer will be negligible (7). Consequently the overall mass transfer coefficient may be approximated by the membrane mass transfer coefficient. Further, since mass transfer is reversible, the membrane mass transfer coefficient is the same for water vapor transport due to osmotic distillation and direct contact membrane distillation.

Since the water vapor flux for direct contact membrane distillation is related to the temperature difference between the strip and feed solutions, the energy flux between the two solutions will determine the required temperature driving force to suppress osmotic distillation. Heat transfer from the strip to the feed solution will occur by conduction through the nonporous section of the membrane as well as through the membrane pores (8). The overall energy flux is given by

$$q = q_m + q_p = \frac{[(1-\varepsilon_m)k_m + \varepsilon_m k_p]}{l} \times (T_s - T_f) = h_m(T_s - T_f) \tag{1}$$

where, q is the overall energy flux, q_m is the energy flux due to heat conduction through the membrane, q_p is the energy flux due to heat transfer through the membrane pores, ε_m is the membrane porosity, l is the membrane thickness, k_m and k_p are the thermal conductivities of the membrane material and the gas in the membrane pores, and h_m is the membrane heat transfer coefficient. The temperatures T_s and T_f represent the temperature at the strip and feed membrane surfaces respectively. Since we aim to suppress water vapor transport, there is no term in Equation (1) for the energy flux due to mass transport of water from the strip to the feed solution. As indicated in Fig. 1, there will be a temperature boundary layer at either surface of the membrane such that

$$q = h_s(T_{sb} - T_s) = h_f(T_f - T_{fb}) \tag{2}$$

where, h_s and h_f are the heat transfer coefficients for the strip and feed temperature boundary layers and T_{sb}, and T_{fb} are the bulk strip and feed temperatures. The overall heat transfer coefficient, U, is given by

$$\frac{1}{U} = \frac{1}{h_s} + \frac{1}{h_m} + \frac{1}{h_f} \tag{3}$$

Thus,

$$q = U(T_{sb} - T_{fb}) \tag{4}$$

These equations will be used when analyzing the experimental data.

EXPERIMENTAL

Polypropylene hollow fiber modules were used in this study. Six hundred hollow fibers were potted in a polycarbonate housing using an epoxy (Guangming Resin Co. Ltd., Wuxi City, P. R. China). The polycarbonate housing had an outside diameter of 2.5 cm and a length of 25.6 cm. The packing density of the hollow fibres was 50%. The polypropylene hollow fibers had an outside diameter of 426 μm, a wall thickness of 45 μm, and an average pore diameter of 0.05 μm, a porosity of 30%, and an effective length of 18 cm. The total membrane area of the module is 1445 cm^2. All chemicals were of analytical grade and used as received. Deionized water was used throughout this study.

Figure 2 is a schematic representation of the experimental setup. The feed was pumped on the shell while the strip solution was pumped inside the lumen of the fibers. The feed and strip were pumped co-currently. As shown in Fig. 2, the feed was recycled to the feed reservoir while the strip was recycled to the strip reservoir. The feed and strip solutions consisted of 500 mL DI water. Feed and strip flow rates were 500 mL min^{-1}. Various amounts of NaCl were added to the strip solution resulting in a final concentration of 1.0, 2.0, 3.0, and 4.0 M. Initial experiments were conducted with the feed and strip solution at the same temperature of 20°C. Consequently, water vapor transferred from the feed to the strip solution. The water flux from the feed to the strip solution was determined by placing the strip reservoir on a balance as shown in Fig. 2.

In a second series of experiments, the strip solution was heated while the feed was maintained at 20°C. Four temperature probes (see Fig. 2)

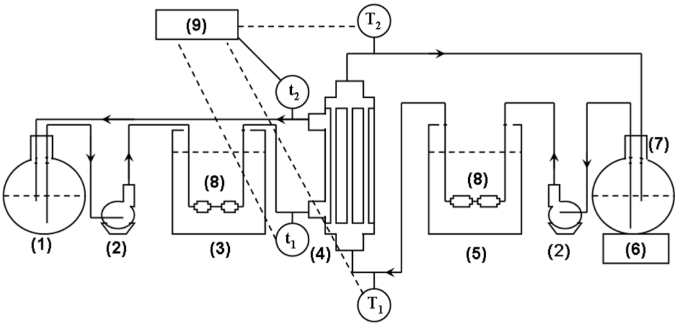

Figure 2. Experimental set up. (1) feed reservoir, (2) feed pump, (3) feed water bath (20°C), (4) membrane module, (5) strip water bath (20–40°C), (6) balance, (7) strip reservoir, (8) glass tube for feed and strip, (9) digital thermometer T_1, T_2, t_1, t_2 temperature sensors.

were used to monitor the feed inlet and outlet and strip inlet and outlet temperatures. The average of the inlet and outlet temperature of the feed and strip were used in analyzing the results. The water vapor flux was determined from the change in weight of the strip reservoir.

RESULTS AND DISCUSSION

The water vapor flux as a function of initial NaCl concentration in the strip solution at 20°C is given in Fig. 3. As the concentration of NaCl increases the water vapor flux increases. Figure 4 gives literature values for the water vapor pressure at various temperatures and NaCl concentrations (9). At equal feed and strip temperatures, increasing the NaCl concentration in the strip solution leads to a decrease in the water vapor pressure. Hence, the water vapor flux increases with increasing NaCl concentration in the strip solution.

Figure 5 gives our experimental data for the variation of water vapor flux with temperature at various NaCl concentrations in the strip. Negative fluxes indicate the transfer of water vapor from the feed to the strip while positive fluxes indicate the transfer of water vapor from the strip to the feed solution. In order to suppress osmotic distillation, the water vapor pressure on both sides of the membrane must be the same. Figure 4 gives literature values for the water vapor pressure. For a

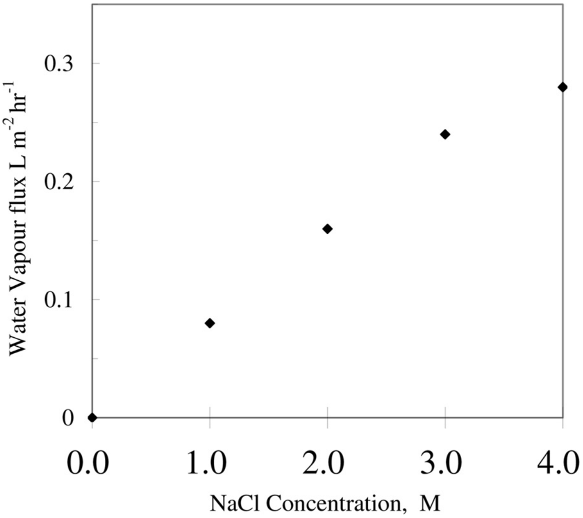

Figure 3. Variation of water flux with NaCl concentration in the strip for feed and strip solutions at 20°C.

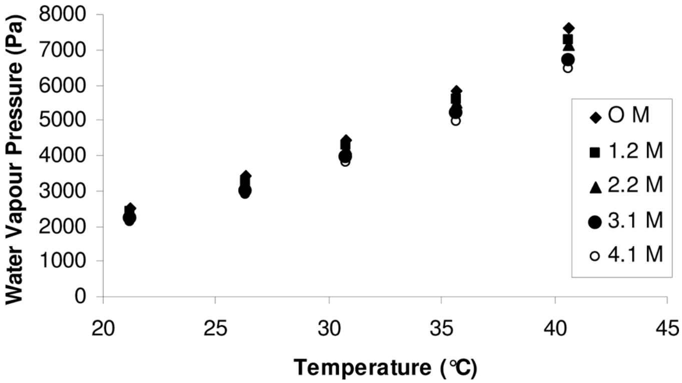

Figure 4. Variation of water vapor pressure with temperature and NaCl concentration.

4.0 M NaCl concentration (open circles in Fig. 4), a very small temperature increase of about 1.5°C is sufficient to obtain the same water vapor pressure as DI water at 20°C. Thus for a strip containing 4.0 M NaCl, if the feed temperature is 20°C a strip temperature of about 21.5°C should be sufficient to equalize the feed and strip side water vapor pressures. However experimentally, Fig. 5 indicates that a temperature difference of about 14°C is required. Thus the required temperature difference is much higher than the difference predicted based on the vapor pressures of the strip and feed solutions.

In direct contact membrane distillation, there will be an energy flux from the hot (here the strip) solution to the cold (here the feed) solution.

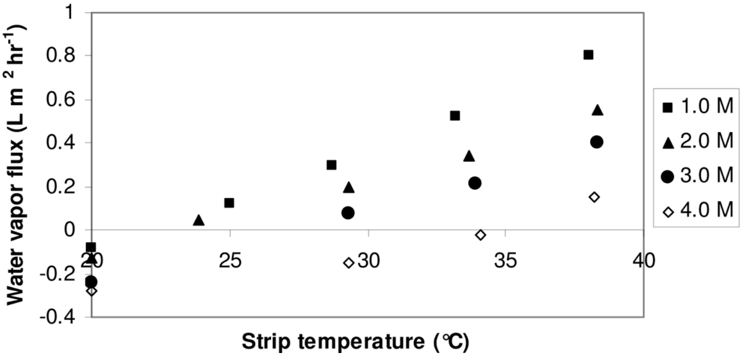

Figure 5. Experimental water vapor flux at various NaCl concentrations and temperatures.

The overall heat transfer coefficient will be given by Eq. (3). The Reynolds number for flow inside the fibers will depend on the temperature and salt concentration of the strip solution. Nevertheless, for strip temperatures between 20°C and 40°C and NaCl concentrations between 0–4 M, the Reyonlds numbers are well below 100 indicating the laminar flow. The entrance length required for a fully developed thermal boundary layer may be approximated by (10).

$$\delta = \sqrt{\frac{1260}{37}\frac{\upsilon x}{v}} \tag{5}$$

where, δ is the thickness of the boundary layer, v is the strip velocity, x is the entrance flow length, and ν the kinematic viscosity. For a flow rate of 500 mL min^{-1}, v is 0.157 m s^{-1}. The entrance length will be greatest for the lowest kinematic viscosity, i.e. strip solution with 0 M NaCl at 40°C. The kinematic viscosity for water at 40°C is 6.58×10^{-7} m^2 s^{-1} (11). Solving Eq. (5) for the entrance length we find the maximum entrance length to be 2.0×10^{-4} m or about 0.2 mm. Equation (5) strictly applies to the thickness of a boundary layer over a flat plate. Thus we use this equation here to approximate the thickness of the boundary layer on the lumen side of a porous tube. Nevertheless, the very small entrance length obtained compared to the length of our hollow fibers suggest that we can assume a fully developed thermal boundary. The lumen side heat transfer coefficient for laminar flow with a fully developed thermal boundary layer and constant surface temperature is

$$Nu = \frac{h_s d}{k_s} = 3.66 \tag{6}$$

where, Nu is the Nusselt number, k_s is the thermal conductivity of the strip solution, and d is the inside diameter of the fibers (12). Equation (6) applies for the Graetz numbers less than 30 where the Graetz number is defined as $d^2 v/\alpha L$, α being the thermal diffusivity of water and L the length of the hollow fibers. For the experimental conditions used here it can be shown that the Graetz number is less than 1. Since the thermal conductivity does not depend strongly on temperature or NaCl concentration over the ranges considered here, we use the thermal conductivity of water at 20°C, 0.606 W m^{-1} K^{-1} (11). Thus the strip side heat transfer coefficient is 6600 W m^{-2} K^{-1}.

The thermal conductivity of polypropylene is 0.138 W m^{-1} K^{-1} (11). The thermal conductivity of water vapor is 0.016 W m^{-1} K^{-1} at 20°C and

$0.019\,\mathrm{W\,m^{-1}\,K^{-1}}$ at 40°C (11). Using the average value over the temperature range 20–40°C, from Eq. (1) the heat transfer coefficient for the membrane is $2260\,\mathrm{W\,m^{-2}\,K^{-1}}$.

For shell and tube hollow fiber modules Wickramsinghe et al. (13) have shown that irregular spacing of the fibers can compromise the rate of mass transfer. These investigators propose the following mass transfer correlation for flow outside and parallel to the fibers.

$$Sh = 1.25\left(\frac{d_e^2 v}{\upsilon L}\right)^{0.93} Sc^{\frac{1}{3}} \tag{7}$$

where, Sh the Sherwood number, d_e equivalent diameter, L is the length of the hollow fiber and Sc the Schmidt number. Replacing the Sherwood number by the Nusselt number and the Schmidt number by the Prandtl number we use this correlation to estimate the heat transfer coefficient on the shell side. We use Equation (7) as it was developed for hollow fiber modules operating at similar conditions to the ones used here. Further Wickramasinghe et al. (13) indicate that analogous heat transfer correlations may be used to develop mass transfer correlations for hollow fiber contactors. The equivalent diameter is 426 μm, and the shell side fluid velocity is $0.097\,\mathrm{m\,s^{-1}}$. Using the kinematic viscosity of water at 20°C, and a Prandtl number for water at 20°C of 7.09, the Nusselt number is 0.28. The shell side heat transfer coefficient is then $384\,\mathrm{W\,m^{-2}\,K^{-1}}$.

From Fig. 4 we estimate a 1.5°C temperature difference between the inside and outside surface of the membrane is required in order to equalize the water vapor pressure across the membrane. From Equation (1) the energy flux is $1.5 \times 2260 = 3390\,\mathrm{W\,m^{-2}}$. From Eq. (3) the overall heat transfer coefficient is $313\,\mathrm{W\,m^{-2}K^{-1}}$. From Equation (4) the temperature difference between the bulk feed and strip solution is 10.8°C. From Fig. 5 the actual temperature difference is about 14°C in reasonable agreement with our prediction.

Unlike membrane distillation, osmotic distillation is often considered an isothermal process. Gostoli (14) however, points out the importance of thermal effects in osmotic distillation. In a recent study Bélafi-Bakó and Koroknai (15) have applied a temperature gradient between the feed and strip solutions in order to enhance the rate of osmotic distillation for fruit juice concentration. Alves and Coelhoso (16) studied mass and heat transfer during osmotic distillation. They also highlight the importance of temperature effects in osmotic distillation. For the experiments conducted here in the absence of an applied temperature gradient, water vapor will transfer from the feed to the strip solution. Vaporization of the feed liquid and condensation of the water vapor at the membrane strip interface, will lead to cooling of the feed liquid and heating of the strip liquid at the membrane surface. Creation of a temperature gradient across the membrane could significantly alter the predicted flux due to osmotic distillation.

In this work, unlike earlier studies, we intentionally impose a temperature gradient across the membrane to suppress water vapor transport. Our results indicate that the actual temperature gradient is much higher than predicted due to the thermal boundary layers in the strip and feed solutions. For cyanide removal, previous investigators have shown that the feed and membrane mass transfer coefficients dominate. The strip mass transfer coefficient is significantly larger than the feed and membrane mass transfer coefficients due to the reaction of the HCN with NaOH (7). Consequently enhancing the rate of mass transfer by increasing the feed side mass transfer coefficient will reduce the temperature difference required between the bulks feed and strip solutions.

In the analysis conducted here we have assumed that there is no mass transfer of water vapor. In fact the establishment of a temperature gradient across the membrane will lead to natural convection of water vapor. However, by carefully controlling the strip temperature it will be possible to minimize transfer of water vapor.

Our results highlight the importance of thermal effects in osmotic distillation which is frequently assumed to be an isothermal process. The results also suggest the possible application of membranes as heat exchangers. In fact Zarkadas and Sirkar (17) describe the feasibility of polymeric hollow fiber heat exchangers for niche applications.

If suppression of osmotic distillation is required in a gas membrane process, the analysis described here could be used to estimate the required temperature gradient and hence the energy costs. Alternatively one could add a non-volatile solute to the solution with the higher water vapor pressure in order to equalize the osmolarity of the strip and feed solutions. However, the addition of a non-volatile solute could lead to complications associated with membrane fouling and the recovery of the solute. The method used to suppress osmotic distillation will depend on the specific application.

Though cyanide removal using gas membranes has been described by a number of previous investigators, for real feed streams water vapor transport by osmotic distillation could affect the viability of the process. While previous investigators (15) have shown that an applied temperature gradient can enhance transport due to osmotic distillation for fruit juice concentration, we use an applied temperature gradient to suppress water vapor transport by osmotic distillation. Our results indicate that the required temperature gradient is much higher than predicted from water vapor pressure data indicating the importance of temperature effects in osmotic distillation.

CONCLUSION

A major practical problem associated with gas membrane based separations is the transfer of the solvent, usually water, from one side of the membrane to the other due to osmotic distillation. We are able to suppress osmotic distillation by imposing a temperature gradient that counters the water vapor pressure gradient created by the two different osmolarities of the feed and strip solutions. The required temperature gradient is larger than predicted by vapor pressure temperature data due to the thermal boundary layers in the strip and feed solutions. Our results highlight the importance of thermal effects in osmotic distillation.

ACKNOWLEDGEMENTS

Funding for this work was provided by the National Science Foundation CBET 0651646.

LIST OF SYMBOLS

d	inside diameter of hollow fibers
d_e	equivalent diameter: four times the cross section for flow divided by the wetted perimeter
h_f	heat transfer coefficient for the feed side temperature boundary layer
h_m	membrane heat transfer coefficient
h_s	heat transfer coefficient for the strip side temperature boundary layer
k_m	thermal conductivity of the membrane material
k_p	thermal conductivity of the gas in the membrane pores
k_s	thermal conductivity of strip solution
ℓ	membrane thickness
L	length of hollow fibers
$\mathrm{N}u$	Nusselt number
Pr	Prandtl Number
q	overall energy flux
q_m	energy flux due to heat conduction through the membrane material
q_p	energy flux due to heat transfer through the pores
Sc	Schmidt number
Sh	Sherwood number
T_f	temperature at the membrane feed interface
T_s	temperature at the membrane strip interface

T_{fb}	bulk feed temperature
T_{sb}	bulk strip temperature
U	overall heat transfer coefficient
v	velocity
x	entrance flow length
α	thermal diffusivity
ε_m	membrane porosity
δ	thickness of the boundary layer
ν	kinematic viscosity

REFERENCES

1. Ho, W.S.W.; Sirkar, K.K. (1992) *Membrane Handbook*; Kluwer Academic Publishers: Dordrecht, The Netherlands.
2. Imai, M.; Furusaki, S.; Miyauchi, T. (1982) Separation of volatile materials by gas membranes. *Ind. Engg. Chem. Process Design & Devel.*, *21* (3): 421.
3. Zhang, Q.; Cussler, E.L. (1985) Hollow fiber gas membranes. *AIChE J.*, *31* (9): 1548.
4. Kenfield, C.F.; Semmens, M.J.; Qin, R.; Cussler, E.L. (1988) Cyanide recovery across hollow fiber gas membranes. *Environ. Sci. Technol.*, *22* (10): 1151.
5. Shen, Z.; Huang, J.; Qian, G. (1997) Recovery of cyanide from wastewater using gas-filled membrane absorption. *Water Environ. Research.*, *69* (3): 363.
6. Shen, Z.; Han, B.; Wickramasinghe, S.R. (2004) Cyanide removal from wastewater using gas membranes: A pilot scale study. *Water Environ. Res.*, *76* (1): 15.
7. Han, B.; Shen, Z.; Wickramasinghe, S.R. (2005) Cyanide removal from industrial wastewaters using gas membranes. *J. Membrane Sci.*, *257* (1–2): 171.
8. Schofield, R.W.; Fane, A.G.; Fell, C.J.D. (1987) Heat and mass transfer in membrane distillation. *J. Membrane Sci.*, *33* (3): 299.
9. Hubert, N.; Gabes, Y.; Bourdet, J.-B.; Schuffenecker, L. (1995) Vapor pressure measurements with a nonisothermal static method between 293.15 and 363.15 L for electrolyte solutions. Applications to the $H_2O + NaCl$ system. *J. Chem. Eng. Data*, *40* (4): 891.
10. Bird, R.B.; Stewart W.E.; Lightfoot, E.N. (1960) *Transport Phenomena*; John Wiley & Sons: New York, NY.
11. Perry, R.H.; Chilton, C.H. (1974) *Chemical Engineers Handbook*, 5th Ed.; McGraw-Hill International Book Company: Tokyo.
12. Incropera, F.P.; DeWitt, D.P. (2002) *Fundamentals of Heat and Mass Transfer*, 5th Ed.; John Wiley & Sons: Hoboken, NJ.
13. Wickramasinghe, S.R.; Semmens, M.J.; Cussler, E.L. (1992) Mass transfer in various hollow fiber geometries. *J. Membrane Sci.*, *69* (3): 235.
14. Gostoli, C. (1999) Thermal effects in osmotic distillation. *J. Membr. Sci.*, *163*: 75.

15. Bélafi-Bakó, K; Koroknai, B. (2006) Enhanced water flux in fruit juice concentration: Coupled operation of osmotic evaporation and membrane distillation. *J. Membr. Sci.*, *269*: 187.
16. Alves, V.D.; Coelhoso, I.M. (2007) Study of mass and heat transfer in osmotic evaporation process using hollow fiber membrane contactor. *J. Membr. Sc.*, *289*: 249.
17. Zarkadas, D.M.; Sirkar, K.K. (2004) Polymeric hollow fiber heat exchangers: An alternative for lower temperature applications. *Ind. Eng. Chem. Res.*, *43* (25): 8093.